Lower Critical Solution Temperature Determination of Smart, Thermosensitive *N*–Isopropylacrylamide-*alt*-2–Hydroxyethyl Methacrylate Copolymers: Kinetics and Physical Properties

Mohammad M. Fares, Ali A. Othman

Department of Applied Chemistry, Jordan University of Science and Technology, P.O. Box 3030, Irbid, Jordan 22110

Received 5 December 2007; accepted 28 February 2008
DOI 10.1002/app.28840
Published online 2 September 2008 in Wiley InterScience (www.interscience.wiley.com).

ABSTRACT: The lower critical solution temperatures (LCSTs) were verified and determined for different molar feed ratios of *N*-isopropylacrylamide (NIPAAm) and 2-hydroxyethyl methacrylate (HEMA) monomers with ultraviolet spectroscopy and differential scanning calorimetry techniques. Increases in the NIPAAm monomer content played a crucial role in the LCST, which increased up to 36.7°C at 50 mol %. However, a further increase in the NIPAAm monomer content steadily reduced the LCST, which decreased to 33°C at 100 mol % NIPAAm [i.e., pure poly(*N*-isopropylacrylamide)]. The rate of copolymerization, assessed by the conventional conversion (%)–time method, and the apparent activation energies were determined. The reactivity ratios of the monomers, determined by the Kelen–Tudos and Fineman–Ross techniques, together with the results of an equation, showed that the copolymer which formed was an alternating copolymer. The *Q*–*e* values for the NIPAAm monomer were determined. The equation showed the linear Arrhenius behavior of $\ln(r_1 r_2)$ versus the reciprocal of the temperature (where r_1 and r_2 are the reactivity ratios of NIPAAm and HEMA, respectively): the activation energy difference [i.e., $(E_{12} + E_{21}) - (E_{11} + E_{22})$, where E_{12}, E_{21}, E_{11}, and E_{22} are various activation energies] was found to be −109 kJ/mol. The copolymers were characterized with ^{1}H-NMR, ^{13}C-NMR, Fourier transform infrared, ultraviolet–visible, thermogravimetric analysis, differential scanning calorimetry, X-ray diffraction, and scanning electron microscopy techniques. J Appl Polym Sci 110: 2815–2825, 2008

Key words: biomaterials; drug delivery systems; hydrophilic polymers; kinetics (polym.); polyamides

INTRODUCTION

In recent years, the synthesis of stimuli-responsive hydrogels has received increasing and crucial importance because of their wide range of uses, such as drug delivery and separation processes.[1–3] These smart hydrogels, which undergo abrupt changes in response to changes in surrounding conditions, such as temperature,[4,5] pH,[6,7] chemicals,[8] photoirradiation,[9] and electric fields,[10] are industrially important. Thermally reversible hydrogels have recently attracted increasing interest in biotechnology for biomedicine.[11] As the temperature of thermosensitive polymer solutions increases, phase separation occurs when the temperature exceeds a definite value; this solution temperature is known as the lower critical solution temperature (LCST), and it is known to be reversible and quite sharp in some cases.

N-alkyl-substituted polyacrylamides that contain hydrophilic and hydrophobic parts in their chemical structures are good examples of polymers that have an LCST in aqueous solutions. The most well known of them, poly(*N*-isopropylacrylamide) [poly(NIPAAm)], exhibits an LCST of about 32°C in an aqueous medium. It assumes a random coil structure (hydrophilic state) below the LCST and a collapsed globular structure (hydrophobic state) above the LCST.[12,13] Furthermore, the closeness of the LCST of poly(NIPAAm) (i.e., ~ 32°C) to the physiological temperature (i.e., 37°C) and the ability to change the LCST value by a copolymerization process have created a fertile area of research for biomedical applications, such as the controlled release of drugs and tissue engineering.[14]

Poly(2-hydroxyethyl methacrylate) [poly(HEMA)] is a favorable biomaterial because of its excellent biocompatibility and physicochemical properties, which are similar to those of living tissues.[15,16] It also exhibits good chemical and hydrolytic stability and good tolerance for entrapped cells. Poly(HEMA) has also been widely used as the backbone for synthesizing stimuli-responsive hydrogels.[17,18]

Correspondence to: M. M. Fares (fares@just.edu.jo).
Contract grant sponsor: Jordan University of Science and Technology (Irbid, Jordan); contract grant number: 43/2007.

The formation of copolymers that may have an LCST is of major importance because of the large contribution of such copolymers to drug delivery systems. Thus, the choice of the *N*-isopropylacrylamide (NIPAAm) monomer, which contains hydrophilic and hydrophobic segments in addition to its good solubility in water, together with the 2-hydroxyethyl methacrylate (HEMA) monomer, which contains mainly hydrophilic moieties, can form a fertile area for tailoring copolymers that can fit onto different site-specific release drugs. Furthermore, the well-known LCST of poly(NIPAAm) at 32°C and the ability to change the LCST value through copolymerization form the basis of this work. Different modified natural and synthetic copolymers have been used in our laboratory to meet the optimum copolymer properties for sustained release studies[19–22] This work was aimed at optimizing the kinetic and physical properties of the formed *N*-isopropylacrylamide-*alt*-2-hydroxyethyl methacrylate (NIPAAm-*alt*-HEMA) copolymer to pave the way for using such systems in the future sustained release of drugs. Thus, the LCST verification of NIPAAm-*alt*-HEMA copolymers with different molar ratios, the rates of copolymerization, and the apparent activation energies were determined. Moreover, the reactivity ratios, determined with the Kelen–Tudos[23] and Fineman–Ross techniques,[24] were investigated in different solvents. Eventually, through eq. (2), the effects of the types of copolymers (i.e., the r_1r_2 value, where r_1 and r_2 are reactivity ratios) on the temperature, which followed Arrhenius behavior, were evaluated.

EXPERIMENTAL

Materials

The monomers NIPAAm (Acros Chemicals Co.) and HEMA (96%; Acros Chemical) were kept in a refrigerator and used as received. *N,N,N′,N′*-Tetraethylenediamine (Sigma–Aldrich), used as an accelerator, was used as received; potassium peroxodisulfate (BDH Chemicals, Ltd.), used as an initiator, was further purified by recrystallization. All solvents and other chemicals were analytical-grade.

Synthesis of NIPAAm-*alt*-HEMA

Various molar feed ratios of NIPAAm to HEMA (0.66, 1.0, 1.3, 1.5, 3.0, and 9.0) were synthesized as follows. Each monomer concentration was dissolved in 25 mL of deionized water, 50% (v/v) water/ethanol, or 50% (v/v) water/acetone. The solutions were sparged with N_2 for 5 min or until the monomer was dissolved. To each solution, 5 mL of 10% (w/w) potassium peroxodisulfate and 5 mL of 10% (w/w) *N,N,N′,N′*-tetraethylenediamine with respect to the total monomer weights were added under an N_2 atmosphere. Then, the mixture was set in a 250-mL, round-bottom flask and sealed under an N_2 atmosphere for 3.5 h in a water bath fixed at 30°C. After the copolymerization was complete, the product was poured into an excess of chloroform, stirred for 15 min, and washed with hot deionized water to remove the homopolymers; it was then filtered and dried in an oven at 80°C for 8–12 h. The samples were further purified via centrifugation. The weight-average molecular weight was determined with a light scattering technique [25]

Phase-transition determination

Cloud-point measurements

A Shimadzu (Japan) UV-2401 spectrophotometer supplied with a heating control device was used to detect the cloud point (or LCST) at $\lambda_{max} = 312$ nm. Each sample was heated from 25 to 50°C at a heating rate of 2°C/min, and the transmittance (%) was monitored. A sudden transmittance (%) decay indicated the formation of turbidity, which was a prestep before precipitation. The cloud point was taken as the midpoint between the onset and end set of the transmittance (%) decay. All measurements were reproducible.

Differential scanning calorimetry (DSC)

A Shimadzu TA-50 differential scanning calorimeter was used to estimate the LCST of each copolymer as the abscissa of the maximum of the endothermic peak. Aluminum pans containing 7 ± 1 mg samples were first heated from 25 to 50°C at a heating rate of 10°C/min, and then a double run was performed after cooling at a heating rate of 2°C/min from 25 to 50°C. The glass-transition temperature was measured first with heating at 50°C/min, then with cooling, and then at a second heating rate of 2°C/min; the glass-transition temperature was taken as the midpoint of the transition.

Instrumentation

^{1}H- and ^{13}C-NMR spectroscopy

The ^{1}H- and ^{13}C-NMR spectra of the copolymers were recorded on a Bruker Biospin spectrometer (400 MHz) in deuterated water and acetone; the samples were macerated in a solvent for 1 day. Chemical shifts (δ) are given in parts per million with tetramethylsilane as an internal standard. The molar ratios of the monomers in the copolymer were determined from the ratio of C-11 (i.e., carbon of the amide group in NIPAAm) to C-12 (i.e., carbon of the ester group in HEMA), which then were used with

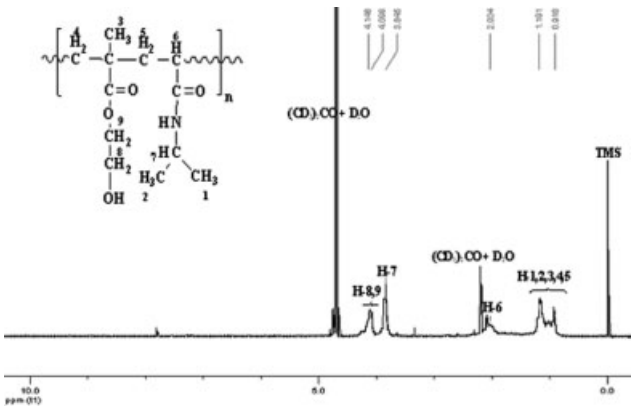

Figure 1 ^{1}H-NMR spectrum of an NIPAAm-*alt*-HEMA copolymer with a molar ratio of 1.0.

Kelen–Tudos and Fineman–Ross techniques to determine the reactivity ratios of the copolymers.

Fourier transform infrared (FTIR) spectroscopy

FTIR spectra were recorded with a Thermo Nicolet (United States) Avator 360 FTIR spectrophotometer in the range of 4000–400 cm^{-1} with KBr pellets. The disks were prepared with a 6% (w/w) sample/KBr powder ratio. The molar ratio of the monomers in the copolymer could be further determined from the ratio of the absorbance of the carbonyl stretching of the amide group of NIPAAm (i.e., at 1646 cm^{-1}) to the absorbance of the carbonyl stretching of the ester group of HEMA (i.e., at 1724 cm^{-1}), and this ratio was conclusively further used to investigate the reactivity ratios of the copolymers.

Thermogravimetric analysis (TGA)

All samples were studied with a Shimadzu TA-50 thermogravimetric analyzer. The decomposition temperature measurements by TGA were carried out on 7 ± 1 mg samples under an N_2 atmosphere at a heating rate of 10°C/min from 25 to 500°C.

X-ray diffraction

X-ray diffraction studies were performed with a Philips-Holland model PW 1729 diffractometer equipped with copper as the target material under the operational conditions of 30 kV, 40 mA, and a wavelength between 1.54060 and 1.54438 Å. The samples were scanned between 5 and 100°.

Scanning electron microscopy (SEM)

SEM images were taken with Polaroid film. The samples in film form were mounted on specimen stubs and coated with gold ions by a sputtering method with a Zeiss (United States) DSM 950 and a Polaron E6100. Electronic absorption spectroscopy was performed with a Unican Helios Alpha apparatus.

RESULTS AND DISCUSSION

Characterization of the NIPAAm-*alt*-HEMA copolymer

^{1}H-NMR, ^{13}C-NMR, and FTIR spectroscopy

Figures 1 and 2 show the ^{1}H-NMR and ^{13}C-NMR spectra of an NIPAAm-*alt*-HEMA copolymer. Figure 3 shows the FTIR spectra of samples with all the molar ratios. The OH stretching located at 3450 cm^{-1} disappeared as the molar ratio changed from 0.66 to 9.0 because of the reduction of the HEMA content in the copolymer.

Thermal analysis and X-ray spectroscopy

Figure 4 presents the TGA and its derivative for an NIPAAm-*alt*-HEMA copolymer with a 1.0 molar

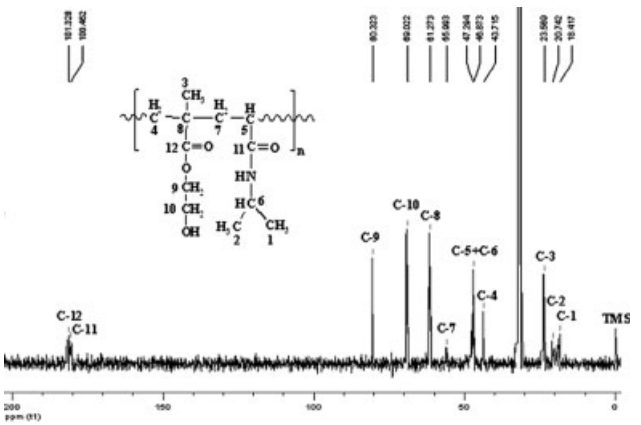

Figure 2 ^{13}C-NMR spectrum of an NIPAAm-*alt*-HEMA copolymer with a molar ratio of 1.0.

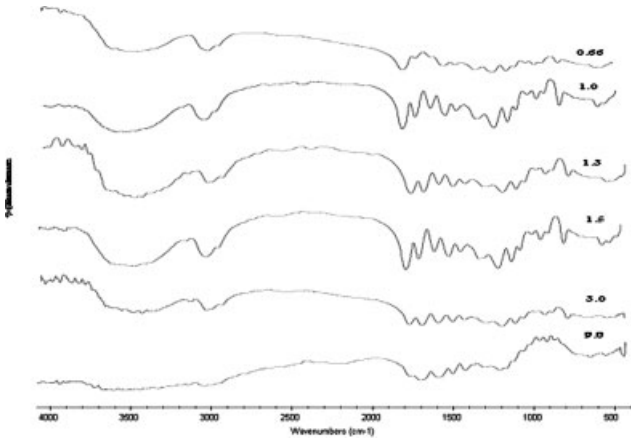

Figure 3 FTIR spectra of NIPAAm-*alt*-HEMA copolymers with different molar ratios.

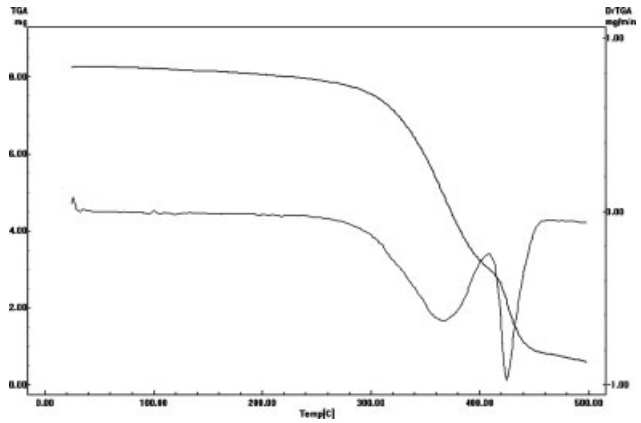

Figure 4 TGA thermogram of an NIPAAm-*alt*-HEMA copolymer with a molar ratio of 1.0.

ratio, which serves as an example for all the sample copolymers. Furthermore, Table I illustrates the thermal parameters determined from each sample, including the decomposition temperatures for the NIPAAm polymer fraction and HEMA polymer and the glass-transition temperatures, as well as the crystallinity (%) of the samples determined from the powder X-ray spectra.

On the basis of the decomposition temperatures of pure poly(NIPAAM) and pure poly(HEMA), the two decomposition temperature peaks appearing for the copolymers could be attributed to NIPAAm and HEMA, respectively. The decomposition temperature of NIPAAm in the copolymers did not change from that of pure poly(NIPAAm), except at the molar ratios of 3.0 and 9.0, whereas all decomposition temperatures of HEMA in the copolymer increased by about 40°C on average with respect to pure poly(HEMA). This shift toward higher temperatures could indicate the presence of NIPAAm segments bonded to HEMA molecules, and so their resistance to temperature was increased; then, the leftover chains of NIPAAm decomposed at nearly the decomposition temperature of pure poly(NIPAAm). At higher molar ratios (i.e., 3.0 and 9.0), small fractions of HEMA segments were incorporated between the larger fraction of NIPAAm, and this caused a decrease in the decomposition temperature of about 15°C (i.e., a 9.0 molar ratio). The glass-transition temperatures at the molar ratios of 0.66, 1.0, and 1.3 were found to be below those of pure poly(NIPAAm) and pure poly(HEMA), and this could indicate that the formation of the copolymer reduced intermolecular and intramolecular forces between chains, reduced the chain alignment, and consequently enlarged the end-to-end distance in these amorphous polymers; at the end, this led to the glass-transition temperature declining. In addition, using higher molar ratios (i.e., 3.0 and 9.0) weakened and diminished the presence of HEMA repeating units in the structure, and thus the glass-transition temperatures increased enough to be close to that of pure(NIPAAm).

The crystallinity (%) of poly(NIPAAm) was 0, as shown in Figure 5 and Table I, and this means that it was totally amorphous, whereas the crystallinity was 11.1% for pure poly(HEMA). The 0.66 molar ratio showed a 100% amorphous system, whereas the 1.0 and 3.0 molar ratios showed very small amounts of crystallinity (i.e., 2.6 and 2.2%). These results indicate that the copolymers which formed did not encourage chain alignment to form crystalline regions because of the larger pendant groups. These pendant groups contained many partially charged atoms, which could be attracted or repelled through intramolecular or intermolecular forces, which then destabilized the chains, caused an expected increase of the end-to-end distance, and consequently diminished the chain alignment and crystallinity. This lack of crystallinity (%) and the consequences explained the large decrease in the glass-transition temperatures of the copolymers.

TABLE I
Thermal Properties of NIPAAm-*alt*-HEMA Copolymers with Different Molar Ratios

Sample	$T_{decomposition}$ (°C)[a]		T_g (°C)[b]	Crystallinity (%)[c]
	NIPAAm	HEMA		
Poly(NIPAAm)	422	—	140	0.0
Poly(HEMA)	—	318	104	11.1
0.66	424	355	92	0.0
1.0	423	367	88	2.6
1.3	422	364	92	—
1.5	426	370	118	—
3.0	414	369	122	2.2
9.0	407	—	134	—

[a] Decomposition temperature derived from the TGA derivative.
[b] Glass-transition temperature derived from DSC.
[c] Derived from X-ray spectra.

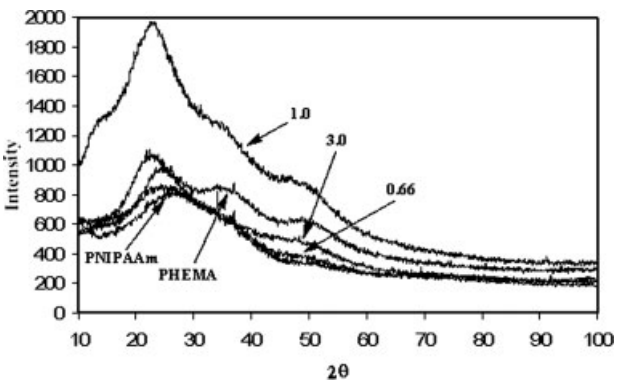

Figure 5 X-ray diffraction patterns of NIPAAm-*alt*-HEMA copolymers with different molar ratios.

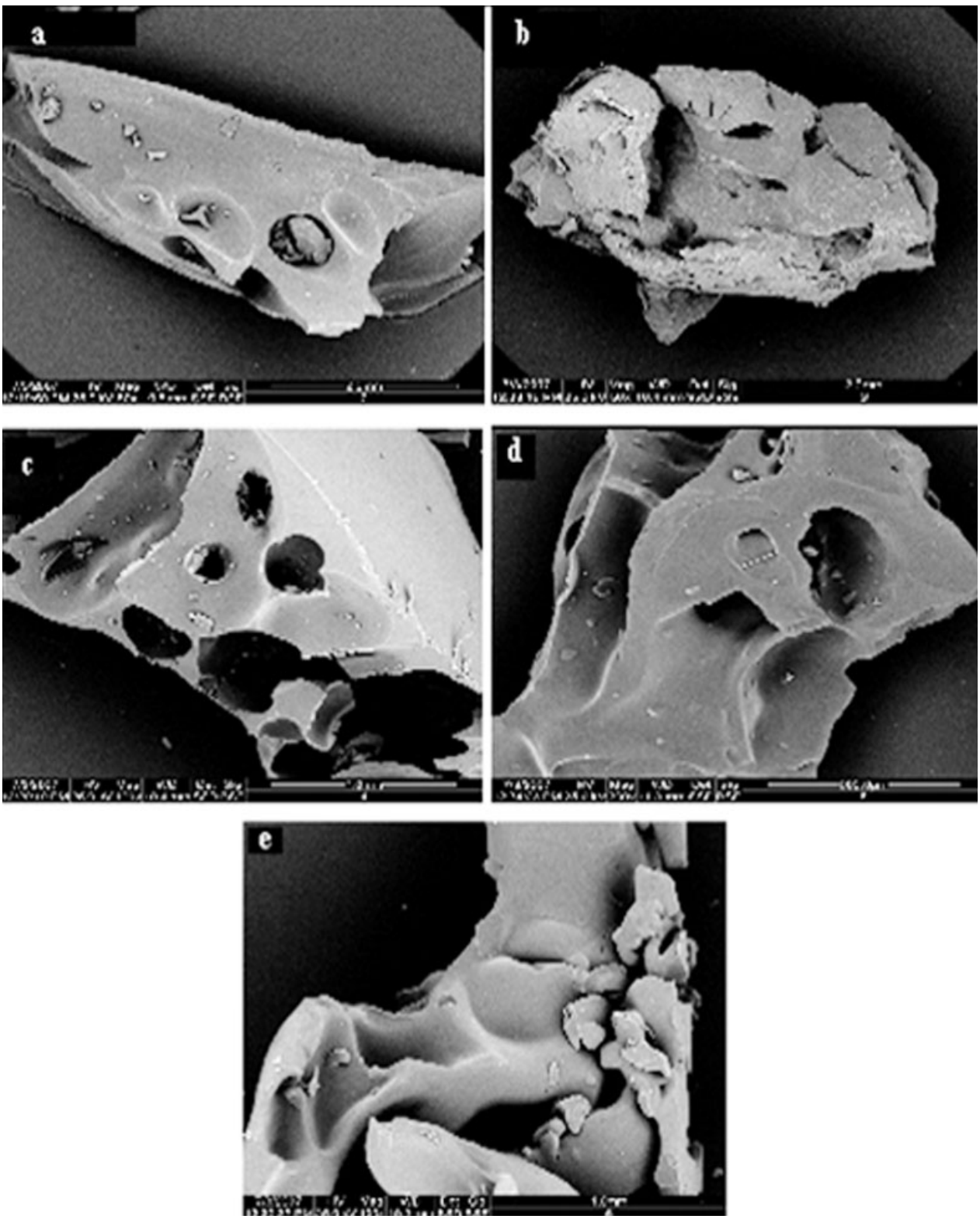

Figure 6 SEM micrographs of (a) poly(NIPAAm), (b) poly(HEMA), (c) an NIPAAm-*alt*-HEMA copolymer with a molar ratio of 0.66, (d) an NIPAAm-*alt*-HEMA copolymer with a molar ratio of 1.0, and (e) an NIPAAm-*alt*-HEMA copolymer with a molar ratio of 3.0.

SEM

The morphology of the copolymers with different molar ratios is shown in Figure 6.

The structures of poly(NIPAAm) and the copolymer with a molar ratio of 0.66, which showed totally amorphous systems, had smooth and slick surfaces

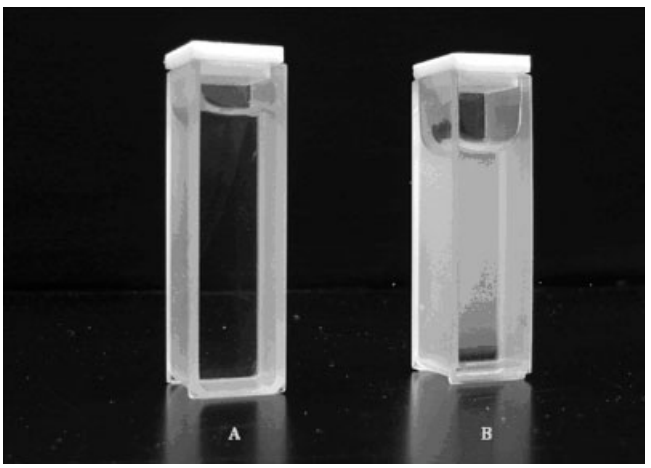

Figure 7 Photographs of an NIPAAm-*alt*-HEMA copolymer with a molar ratio of 9.0 (A) before reaching LCST and (B) after reaching LCST.

with a hole diameter of around 300–500 μm, whereas the copolymers with molar ratios of 1.0 and 3.0, which previously showed very low crystallinity (%), showed a two-dimensional slippery aggregate structure with holes of 250–500 μm. Partially crystalline poly(HEMA) (i.e., crystallinity = 11.1%) showed flaked, rocky structures that contained some oriented cracks, which resembled the crystalline region in poly(HEMA). The amorphous structure of the samples and hence the rocky aggregate structures did not allow further investigation of the outer morphological structures.

Phase-transition determination

Cloud-point measurements

The cloud point is the point at which a solution turns from transparency (i.e., quite soluble) into a turbid solution (i.e., partially soluble) as a result of a phase-transition change, which eventually leads to precipitation. This phase change takes place at a certain temperature called the LCST. Loh et al.[26] suggested a mechanism of phase separation that takes place at LCST. It assumes that at a certain temperature (i.e., the LCST), the copolymer changes its conformation; consequently, polymer–polymer interactions become much more favorable than polymer–water interactions, and a polymer aggregates forms that eventually leads to phase separation.

Using ultraviolet spectroscopy, one can detect an abrupt change in the transmittance (%) at elevated temperatures: a sudden drop in the transmittance (%) at a certain temperature takes place as a result of solution turbidity (i.e., phase separation), and then the LCST is detected. Figure 7 shows a photograph of a polymeric solution before and after it reaches the LCST.

The control of the LCST of a copolymer can be accomplished through the adjustment of the relative hydrophobicity of the copolymer. Thus, the LCSTs for copolymers of different molar ratios with increasing hydrophobicity (i.e., 0.66, 1.0, 1.3, 1.5, 3.0, and 9.0) as well as pure poly(NIPAAm) and pure poly (HEMA) were investigated. The change in the transmittance (%) with increasing temperature for the samples is shown in Figure 8. Furthermore, the determined LCSTs are plotted versus the NIPAAm content (mol %) in Figure 9.

These two figures show that the LCST first increased from 35°C for pure poly(HEMA) to 36.7°C for 50 mol % NIPAAm, and then it sharply declined exponentially to 33°C, which is the LCST of pure poly(NIPAAm). It is known that NIPAAm contains hydrophobic and hydrophilic groups, whereas poly (HEMA) contains only hydrophilic groups. Thus, the increase shown in Figure 3 is due to the presence of more hydrophilic groups in the copolymer on account of the larger HEMA fraction, whereas as the content of NIPAAm increased, a decline in the LCST values was noticed because of the increase in the

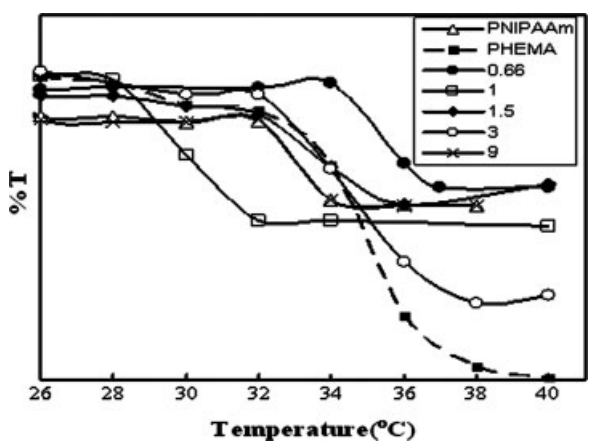

Figure 8 Change in the transmittance (%) versus the temperature.

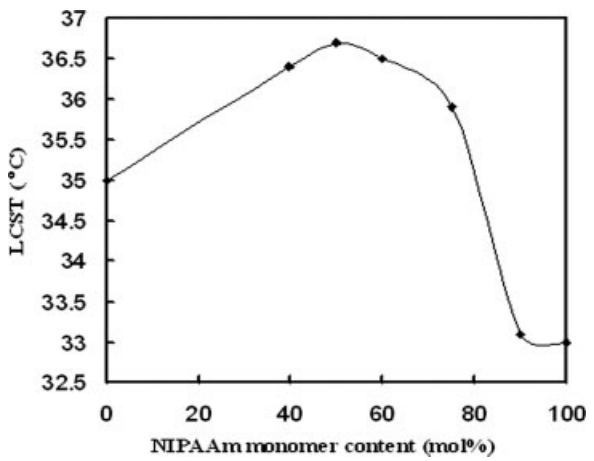

Figure 9 Changes in LCST with the NIPAAm monomer content (mol %).

hydrophobicity of the copolymer, which encouraged the copolymer to depart from the solution at lower temperatures. Thus, the LCST can be controlled through the adjustment of the fraction of hydrophobicity in the copolymers that are formed, and consequently, the temperature at which the copolymers can dissolve or precipitate can be controlled. This fact is very important for drug delivery and site-specific release applications.

DSC

Conventional DSC provides information about the overall heat flow measured as a function of temperature or time. It has been reported that the sharpness of the phase transition of copolymers becomes very low with increasing comonomer content (i.e., HEMA in our case) with respect to the very sharp transition for aqueous solutions of poly(NIPAAm).[27] This can be seen in Figure 10, in which the LCST is indicated by an arrow. The molar ratio of 9.0 shows a clear endotherm of the LCST at 33°C, whereas the other molar ratios show a loss of sharpness of the phase transition.

Thus, the random endotherm oscillations in the thermogram, which then confuse the determination of the LCST, require deconvolution of peak overlapping through more sophisticated and modulated DSC techniques (of which we were not capable), and the determination of the LCST was conclusively monitored via ultraviolet spectroscopy, as mentioned previously, and then fitted to the conventional DSC thermogram in Figure 10.

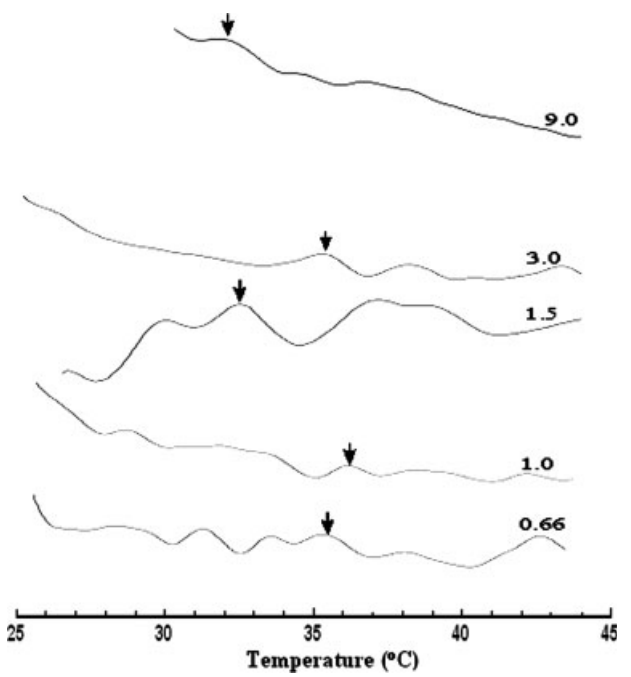

Figure 10 DSC thermograms of NIPAAm-*alt*-HEMA copolymers with different molar ratios.

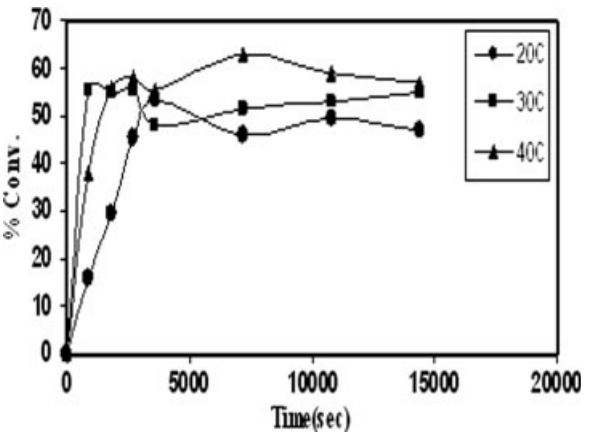

Figure 11 Conversion (%) versus time for a molar feed ratio of 1.0 at different temperatures.

Kinetic analysis

The study of some kinetic parameters such as the rate of copolymerization and the apparent activation energy illuminates a molecular-level investigation of the effects of two monomers competing with each other to enter a chain headed by an M_1 or M_2 radical. Thus, conventional plots of the conversion (%) versus time were plotted in the temperature range of 20–40°C (Fig. 11). The rate of polymerization was determined from the non-steady-state curve. Table II summarizes the kinetic parameters deduced directly from the conversion (%)–time plot for the copolymers of different molar ratios.

Table II shows that the rate of polymerization, calculated from the slope of the conversion (%) versus time, increased as the temperature increased for all copolymer molar ratios, which necessarily showed Arrhenius behavior, and eventually the apparent activation energy could be calculated through an Arrhenius relationship. Furthermore, as the molar ratio increased (i.e., the NIPAAm monomer increased), the apparent activation energy increased, and this emphasized that the NIPAAm monomer could favor and more easily interact with the HEMA monomer than itself. This preference and the higher activation energy were reflected quite clearly in the molecular weight of the copolymer. Because the polymerization time was fixed at 3.5 h and the activation energy was larger at larger NIPAAm contents, the entrance rate of the NIPAAm monomer into the chain became slower; consequently, the molecular weight at the end of the polymerization process was less. This could be clearly seen through the large molecular weight at the molar ratio of 0.66 (i.e., 1,400,000), which became 110,000 at the molar ratio of 3.0. Thus, the increase in the NIPAAm content in the copolymer conclusively caused a higher activation energy and a lower average molecular weight, and it further reflected the alternating behavior of

TABLE II
Kinetic Parameters of NIPAAm-*alt*-HEMA Copolymers with Different Molar Ratios

Molar ratio	Temperature (°C)	Time (min)	Yield (%)	R_p (g/L s)[a]	E_a (kJ/mol)[b]	M_w[c]
0.66	20	15	00.38	0.0808	7.90	
		30	11.28			
		45	12.38			
		60	18.53			
	30	15	26.53	0.2260		1,400,000
		30	36.04			
		45	37.87			
		60	30.18			
	40	15	12.97	0.0940		
		30	14.52			
		45	18.75			
		60	22.74			
1.0	20	15	16.17	0.2917	23.34	
		30	29.31			
		45	45.74			
		60	53.66			
		30	54.87			330,000
		45	55.40			
		60	48.24			
	40	15	38.15	0.5432		
		30	55.97			
		45	58.22			
		60	55.62			
3.0	20	15	12.05	0.4277	11.40	
		30	28.66			
		45	38.03			
		60	38.83			
	30	15	15.00	0.4307		110,000
		30	12.76			
		45	20.24			
		60	24.13			
	40	15	12.96	0.5841		
		30	14.52			
		45	18.74			
		60	22.73			
9.0	20	15	07.80	0.7440	17.70	
		30	16.19			
		45	25.89			
		60	29.14			
	30	15	11.34	0.9341		
		30	20.37			
		45	50.68			
		60	49.94			
	40	15	18.59	1.1904		
		30	16.16			
		45	18.97			
		60	15.59			

[a] Rate of copolymerization.
[b] Activation energy.
[c] Weight-average molecular weight determined by a light scattering technique.[25]

the copolymer from the NIPAAm monomer to the HEMA monomer.

Reactivity ratios

The reactivity ratios of the copolymer were thoroughly determined with two techniques, Kelen–Tudos, and Fineman–Ross, in three different solvents: water, 50% (v/v) water/ethanol, and 50% (v/v) water/acetone. The experimental molar ratios were determined with ^{13}C-NMR through the intensity ratio of C-11 to C-12 (see Fig. 1) and with FTIR spectroscopy through the ratio of the absorbance of CO (amide) in NIPAAm (i.e., at 1724 cm^{-1}) to the

absorbance of CO (ester) in HEMA (i.e., at 1646 cm^{-1}). For greater convenience, the molar ratios were further calculated and compared with the experimentally determined value through the following relation.[25]

$$F_1 = \frac{r_1 f_1^2 + f_1 f_2}{r_1 f_1^2 + 2 f_1 f_2 + r_2 f_2^2} \quad (1)$$

where F_1 is the molar ratio and f_1 is the molar ratio in the feed. The use of three different solvents was meant to confirm the reactivity ratio determinations. Furthermore, with the Alfrey–Price relationship,[28] the Q and e values were determined for the NIPAAm monomer. Table III illustrates the physical properties of the different molar ratios in the feed in different solvents. The agreement of the calculated molar ratios and the experimental molar ratios determined by ^{13}C-NMR and FTIR spectroscopy with the three different solvents was very good and confirmed the accuracy of the results. This accuracy was reflected in the determination of the reactivity ratios for NIPAAm (r_1) and HEMA (r_2), as Table III suggests, where r_1 shows a very clear-cut alternating behavior of the NIPAAm monomer toward the HEMA monomer, whereas HEMA showed random behavior toward NIPAAm. This could be seen in the series for both techniques. In both techniques, the product of $r_1 r_2$ confirmed that the copolymer was an alternating type. An investigation of the numerical r_1 and r_2 values confirmed that the alternating behavior was from the NIPAAm monomer only. Thus, the copolymer sequence probably consisted of a large sequence of alternating repeating units with some randomness, especially when the content of HEMA was larger in the copolymer.

The Q value in the Alfrey–Price equation represents the reactivity or resonance stability of the macroradical ($M_1^\bullet$) of the double bond as a result of the withdrawal or release of electrons to or away from the double bond. Higher Q values indicate a larger release of electrons to the double bond from pendant conjugated groups (i.e., higher reactivity), whereas lower Q values indicate a larger withdrawal of electrons away from the double bond to the pendant groups. The e value in the Alfrey–Price equation represents the polarity of the monomer in question. Higher e values indicate greater electron-withdrawing power of the α substituents on the vinyl monomer and hence greater partial charges on the monomer. The Q–e values for our desired NIPAAm monomer were determined with the two techniques and different solvents. Table III shows that the Q values were around 2.0 in water and water/ethanol solvents. Such Q values for NIPAAm in comparison with similar structures that have electron-conjugated pendant groups such as benzyl methacrylate (Q = 3.64) and other monomers[24] reflect that NIPAAm monomer reactivity can be classified as moderate. Furthermore, the NIPAAm monomer has higher polarity than the standard styrene monomer ($e = -0.8$), whereas it is less polar than methacrylamide (e = 2.24). The partial charges on the functional groups, which can cause polarity on the NIPAAm monomer, can probably lead to weakened intramolecular and intermolecular forces between chains and thus impose a lower glass-transition temperature, reduce the crystallinity (%), and increase polymer amorphous behavior.

It is further known that the Q–e values are dependent on the $r_1 r_2$ product, so if any error in this product exists, it will be directly reflected in the accuracy of the Q–e values. The determination of $r_1 r_2$ product values with different solvents and different techniques was meant to narrow the error range and thus to determine the Q–e values to the greatest accuracy; thus, our data were found to be in accordance with literature values.[29]

Kinetic parameter $r_1 r_2$

Equation (2) was investigated[30] to correlate the $r_1 r_2$ product exponentially with the temperature as follows:

$$r_1 r_2 = \frac{A_{11} A_{22}}{A_{12} A_{21}} \exp\left(\frac{(E_{12} + E_{21}) - (E_{11} + E_{22})}{RT}\right) \quad (2)$$

where E_{12} is the activation energy of monomer 2 needed to join the $M_1^\bullet$ macroradical chain and E_{21} is the activation energy of monomer 1 needed to join the $M_2^\bullet$ macroradical chain. Furthermore; E_{11} is the activation energy of monomer 1 needed to join the $M_1^\bullet$ macroradical chain, and E_{22} is the activation energy of monomer 2 needed to join the $M_2^\bullet$ macroradical chain. If $\ln(r_1 r_2)$ in eq. (2) is plotted versus the reciprocal of the temperature in kelvins ($1/T$), the overall activation energy, $\Delta E = (E_{12} + E_{21}) - (E_{11} + E_{22})$, can be determined. Table IV illustrates changes in the $r_1 r_2$ product with temperature changes that were determined with the Kelen–Tudos technique.

Figure 12 shows the linear relationship of $\ln(r_1 r_2)$ versus $1/T$, which is derived from eq. (2). The overall activation energy [i.e., $(E_{12} + E_{21}) - (E_{11} + E_{22})$] was found to be −109 kJ/mol. This value confirms $(E_{12} + E_{21}) \ll (E_{11} + E_{22})$; consequently, monomer 1 prefers interacting with the $M_2^\bullet$ macroradical chain, and monomer 2 prefers interacting with the $M_2^\bullet$ macroradical chain. This conclusively confirms the alternating behavior of the monomers toward each other.

TABLE III
Physical Properties of the NIPAAM-*alt*-HEMA Copolymers

			Kelen–Tudos							Fineman–Ross						
			F_1							F_1						
Solvent	ε[a]	f_1[b]	Experimental[c]	Calculated[d]	r_1	r_2	r_1r_2	Q_1	e_1	Experimental[c]	Calculated[d]	r_1	r_2	r_1r_2	Q_1	e_1
H_2O	78				0.0509	0.427	0.0217	2.04	1.58			0.0203	0.3896	0.0079	1.94	1.81
		0.66	0.36	0.39						0.37	0.39					
		1.0	0.40	0.42						0.40	0.42					
		1.3	0.42	0.44						0.42	0.44					
		1.5	0.41	0.46						0.41	0.45					
		3.0	0.43	0.50						0.43	0.48					
		9.0	0.43	0.58						0.43	0.53					
H_2O/ethanol [50% (v/v)]	51.4				0.0150	0.273	0.0040	2.61	1.96			0.0296	0.4048	0.0121	1.94	1.71
		0.66	0.43	0.42					0.40	0.39						
		1.0	0.42	0.44						0.39	0.42					
		1.3	0.43	0.41						0.44	0.40					
		1.5	0.43	0.47						0.41	0.45					
		3.0	0.44	0.49						0.42	0.49					
		9.0	0.45	0.52						0.44	0.55					
H_2O/Acetone [50% (v/v)]	49.7				0.0332	0.135	0.0045	5.31	1.94			0.0144	0.1468	0.0021	4.57	2.09
		0.66	0.47	0.52						0.46	0.45					
		1.0	0.47	0.53						0.46	0.47					
		1.3	0.47	0.54						0.47	0.48					
		1.5	0.47	0.55						0.47	0.48					
		3.0	0.48	0.60						0.47	0.50					
		9.0	0.48	0.71						0.47	0.53					

[a] Dielectric constant at 25°C. For mixtures, the relation $\varepsilon = (\varepsilon_1 + \varepsilon_2)/2$ was used.
[b] The molar ratio in the feed.
[c] The experimental molar ratio determined from ^{13}C-NMR and FTIR spectroscopy.
[d] The molar ratio calculated with eq. (1).

TABLE IV
Changes in the r_1r_2 Product with Temperature Changes for the NIPAAm-*alt*-HEMA Copolymers

Temperature (°C)	r_1	r_2	r_1r_2
20	0.0034	0.114	0.0003876
30	0.0509	0.427	0.0217343
40	0.0356	0.178	0.0063368

CONCLUSIONS

The synthesis, characterization, and physical and kinetic properties of thermosensitive NIPAAm-*alt*-HEMA copolymers were studied. Several conclusions were drawn:

- The LCST of various NIPAAm-to-HEMA molar ratios first increased as result of increasing NIPAAm content from 35°C [pure poly(HEMA)] to a maximum value of 36.7°C at 50 mol % NIPAAm, and then it declined to 33°C, the LCST of pure poly(NIPAAm). This behavior was attributed to the increase in the hydrophobicity as the NIPAAm content (mol %) increased, and consequently, the ability of water molecules to dismiss polymer chains from the solution at lower temperatures increased.
- The increase in the molar feed ratio could affect several features of the formed copolymers; for example, it could increase the activation energy and reduce the molecular weight. The alternating behavior preference from the NIPAAm monomer side caused large increases in the activation energy values. Consequently, the presence of a larger NIPAAm content caused a dramatic decrease in the molecular weight of the copolymer because of the delay of the interaction of the NIPAAm monomer with the NIPAAm macroradical in comparison with the HEMA monomer.
- The reactivity ratios determined with the Kelen–Tudos and Fineman–Ross techniques in different solvents, in addition to results from eq. (2), demonstrated that the copolymer which formed was alternating with some random segments. The *Q*–*e* values for the NIPAAm monomer were in accordance with similar literature values for acryl amide.

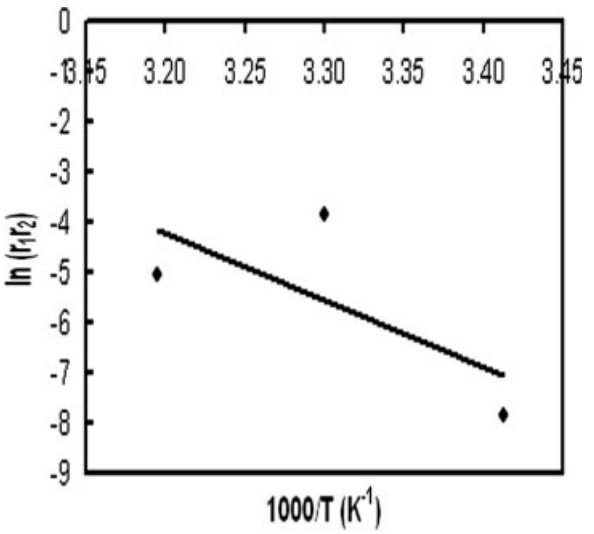

Figure 12 Changes in $\ln(r_1r_2)$ versus $1000/T$.

References

1. Langer, R.; Peppas, N. A. AIChE J 2003, 49, 2990.
2. Zhang, X. Z.; Wu, D. Q.; Chu, C. C. Biomaterials 2004, 25, 3793.
3. Jeong, B.; Gutowska, A. Trends Biotechnol 2002, 20, 305.
4. Ricka, J.; Tanaka, T. Macromolecules 1984, 17, 2916.
5. Hirokawa, Y.; Tanaka, T. J Chem Phys 1984, 81, 6379
6. Grignon, J.; Scallan, A. M. J Appl Polym Sci 1980, 25, 2829.
7. Hoffman, A. S. J Controlled Release 1987, 6, 297.
8. Ishihara, K.; Muramoto, N.; Shinohara, I. J Appl Polym Sci 1984, 29, 211.
9. Kungwatchakun, D.; Irie, M. Makromol Rapid Commun 1988, 9, 243.
10. Eisenberg, S. R.; Grodzinski, A. J. J Membr Sci 1984, 19, 173.
11. Berna, Y.; Belma, I.; Mehmet, K. Eur Polym J 2002, 38, 1343.
12. Alarcon, C. D. L.; Pennadam, S.; Alexander, C. Chem Soc Rev 2005, 34, 276.
13. Zhang, X. Z.; Yang, Y. Y.; Chung, T. S.; Ma, K. X. Langmuir 2001, 17, 6094.
14. Zhang, W.; Shi, L.; Wu, K.; An, Y. Macromolecules 2005, 38, 5743.
15. Brahim, S.; Narinesingh, D.; Elie, A. G. Biomacromolecules 2003, 4, 497.
16. Lahooti, S.; Sefton, M. V. Tissue Eng 2000, 6, 165.
17. Kou, J. H.; Fleisher, D.; Amidon, G. L. J Controlled Release 1990, 12, 241.
18. Albin, G.; Horbett, T. A.; Miller, S. R.; Ricker, N. L. J Controlled Release 1987, 6, 267.
19. Fares, M. M.; El-Faqeeh, A. S.; Osman, M. E. J Polym Res 2003, 10, 119.
20. Fares, M. M.; El-Faqeeh, A. S. J Therm Anal Calorim 2005, 82, 161.
21. Fares, M. M.; Al-Ta'ani, B. Acta Chim Slov 2003, 50, 275.
22. Fares, M. M. J Polym Mater 2003, 20, 75.
23. Kelen, T.; Tudos, J Macromol Sci Chem 1975, 9, 1.
24. Fineman, M.; Ross, S. D. J Polym Sci 1950, 5, 259.
25. Carraher, C. E. Polymer Chemistry, 6th ed.; Marcel Dekker: New York, 2003; p 82.
26. Loh, W.; Da Silva, R. C. J Colloid Interface Sci 1998, 202, 385.
27. Eeckman, F.; Moes, A. J.; Amighi, K. Eur Polym J 2004, 40, 873.
28. Alfrey, T., Jr.; Price, C. C. J Polym Sci 1947, 2, 101.
29. Brandrup; Immergut, E. H.; Grulke, E. A. Polymer Handbook, 4th ed.; Wiley: New York, 1999; pp 81 and 309.
30. Fares, M. M. Open Macromol J 2008, 2, 1.